Karaj branch

Journal of Applied Chemical Research
jacr.kiau.ac.ir

Journal of Applied Chemical Research, 12, 2, 17-29 (2018)

Fluorene Functionalized Nanoporous SBA-15 as a Novel Adsorbent for Fast and Efficient Removal of Acid Dyes

Mona Hajialifard[1], Leila Hajiaghababaei[1*], Alireza Badiei[2], Marzieh Yadavi[2], Shiva Dehghan Abkenar[3], Mohammad Reza Ganjali[4], Ghodsi Mohammadi Ziarani[5]

[1]Department of Chemistry, Yadegar -e- Imam Khomeini (RAH) Shahre Rey Branch, Islamic Azad University, Tehran, Iran

[2]School of Chemistry, College of Science, University of Tehran, Tehran, Iran

[3]Department of Chemistry, Savadkooh Branch, Islamic Azad University, Savadkooh, Iran

[4]Center of Excellence in Electrochemistry, Faculty of Chemistry, University of Tehran, Tehran, Iran

[5]Department of Chemistry, Alzahra University, Tehran, Iran

(Received 14 Jun. 2017; Final version received 12 Sep. 2017)

Abstract

SBA-15 grafted with N-(4-(trimethylsilyl) butyl)-9H-fluorene-9-amine was synthesized by a simple strategy and applied to removal of Acid Red 33 and Acid Black 194 from aqueous solutions. SBA-15 was synthesized and Functionalized according to procedure in the literature. Fluorene functionalized SBA-15 was showed the BET surface area 200 m^2g^{-1} and pore diameter 4.2 nm, based on adsorption-desorption of N_2 at 77 K. The presence of organic groups in the silica framework was demonstrated by FTIR and Raman spectrum. The effects of pH, amount of adsorbent, contact time and dye concentration on adsorption were determined in order to find the optimum adsorption conditions. The data fitted well to the Langmuir model with maximum adsorption capacities 500.0 mg/g for Acid Red 33 and 110.0 mg/g for Acid Black 194. The results were shown that this methodology could be suitable for the removal of the pollutant acid dyes from dyeing wastewater of handmade carpet's fibers.

Keywords: *Dye removal, Acid red 33, Acid black 194, N-(4-(trimethylsilyl)butyl)-9H-fluorene-9-amine functionalized SBA-15.*

[*]***Corresponding author:*** *Leila Hajiaghababaei, Department of Chemistry, Yadegar -e- Imam Khomeini (RAH) Shahre Rey Branch, Islamic Azad University, Tehran, Iran. E-mail: lhajiaghababaei@yahoo.com, Tel:+989125017614.*

Introduction

Organic dyes are widely used in various fields but they are major pollutants in aqueous solutions too. Most industrial dyes have undesirable properties such as toxicity and mutagenesis [1] and unfortunately most of them are stable and resistance to photo degradation, biodegradation and oxidizing agents [2]. Acid dyes are used in many industries such as textile, paper, food processing, cosmetics, plastics, printing, leather, pharmaceutical and dye manufacturing. Water pollution caused by industrial wastewater has become a common problem for many countries [3].

Currently, several physical or chemical processes are used to treat dye-laden wastewaters, such as adsorption [4-6], chemical oxidation [7], electrochemical oxidation [8], and photocatalytic oxidation [9]. Most of dyes are stable to photo-degradation, bio-degradation and oxidizing agents [10]. Therefore, the adsorption process is one of the high efficient and low cost methods to remove dyes from water and wastewater. Nowadays different adsorbents like activated carbons, clays, ion exchange resins and zeolites have been investigated to removal of dyes [11-13]. But, highly porous materials offer a number of potential advantages as adsorbents including larger pore volume and diameter, high surface area and regular channel type structures. It is also possible to manipulate these properties so as to suit those of the adsorbent [14]. The development of functionalized mesoporous materials for adsorption applications including the removal and determination of metal ions [15-17], organics[18], dyes[19-23], radio nuclides [24], and anionic complexes[25, 26], has generated a considerable interest. For adsorption processes, a variety of functional groups can be grafted or incorporated on the surface of mesoporous channels and prepare highly effective adsorbents [27, 28].

In 1998, Zhao et al. [29] synthesized a new type of mesoporous material called SBA, with uniform hexagonal structure. One member of the mesoporous molecular sieves SBA family is SBA-15. It is a highly ordered material possessing a regular two dimensional hexagonal array of channels. This material typically has a pore diameter of the order of 7–10 nm. This study examines the potential of SBA-15 grafted with N-(4-(trimethylsilyl)butyl)-9H-fluorene-9-amine (fluorene functionalized SBA-15) (Figure 1.a) as a new adsorbent for removing of acidic dyes. In order to, the functionalized SBA-15 was prepared and characterized. The fluorene functionalized SBA-15 was applied to removal of Acid Red 33 (AR 33) (Figure 1.b) and Acid Black 194 (AB 194) (Figure 1.c) from the aqueous solution. The applicability of this adsorbent was evaluated in view of the effects of solution pH, adsorbent dosage and contact time.

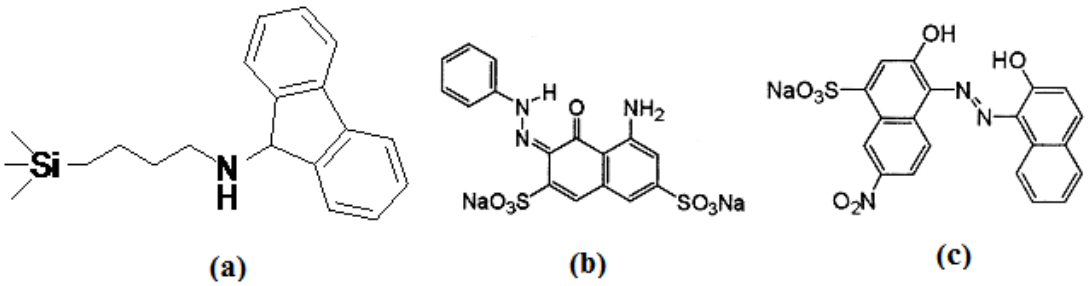

Figure 1. The structure of fluorene functionalized SBA-15(a), Molecular structure of dyes Acid red 33(b), Acid black 194(c).

Experimental

Instrumentation

FT-IR spectra were obtained on Equinox 55 spectrometer. Raman spectra were obtained on SENTERRA spectrometer. Small and wide angle x-ray scattering (XRD) patterns were recorded with a model Hecus S3-MICROpix SAXS diffractometer with a one-dimensional PSD detector using Cu Kα radation (50KV, 1mA) at wave length 1.542 A°. Thermogravimetric analysis (TGA) was performed on a TA Q50 instrument. The scans were performed between 25 and 800 °C at 10 °C/min. Elemental analyses was carried out by a Rapid elemental analyzer. Nitrogen physisorption isotherms were obtained on a BELSORP mini-II at liquid nitrogen temperature (77K). Surface area was measured using the Brunauer-Emmett-Teller (BET) method, pore size distributions were calculated from the nitrogen isotherms by Barrett-Joyner-Halenda (BJH) method. The pH was controlled by Metrohm pH-meter model 713 and Shimadzo 25 double beam spectrophotometer was used for the detection of dye concentration in the solution.

Reagents and solutions

P123 ($EO_{20}PO_{70}EO_{20}$, MW=5800) was obtained from Aldrich. Fluorene, bromine, carbon tetrachloride, tetraethylorthosilicate (TEOS), γ-(amino propyl)triethoxysilane (APTES) Sodium hydroxide and hydrochloric acid were obtained from Merck (Germany). Toluene was dried according to the standard purification methods [30]. Acid Red 33 (AC33) and Acid Black 194 (AB194) were purchased from Bayer (Germany). All the reagents were of analytical grade and used as received without further purification. Double distilled water (DDW) was used throughout the study. The stock solutions of dyes were prepared by dissolving dye powder in DDW. The stock solution was then diluted to prepare the desired concentration of dye solutions. All glassware were soaked in dilute nitric acid for 12 h and finally rinsed for three times with DDW prior to use.

Synthesis of SBA-15 grafted with N-(4-(trimethylsilyl)butyl)-9H-fluorene-9-amine

SBA-15 material was synthesized by following the procedure reported at literature [31-33]. Aminopropyl functionlized SBA-15 material was synthesized by following the procedure reported by Zhao et al. [33]. 2 g Aminopropyl functionlized SBA-15 was placed under vacuum for 30 min, then 80 mL dry toluene was added and stirred for 15 min, 9-Bromofluorene [34] (1.11 g, 4.5 mmol) was added to the resulting mixture under inert atmosphere (Ar) and reflux for 24 h. Then it was cooled at room temperature and toluene was removed by filtration under vacuum. It was dried at room temperature and functionalized silica was washed with ethanol by using a soxhlet apparatus for 3 days, followed by drying at room temperature to remove ethanol.

Dyes removal experiment

For each experimental run, ten milligram of fluorene functionalized nanoporous silica SBA-15 were added to 10 mL of 50 mg L^{-1} of each of acidic dyes solutions with predetermined concentration. The mixed solution was gently shacked at room temperature for 5 min. At the end of the adsorption period, the supernatant was centrifuged for 2 min at 3750 min^{-1}. The residual amounts of dyes in the solution were determined spectrophotometrically at 530 and 573 nm for Acid Red 33 (AR 33) and Acid Black 194 (AB 194), respectively.

All the experiments were performed at room temperature. The effects of pH, contact time and dye concentration on adsorption were investigated. For adsorption isotherm, the dye solution of different concentration in the range of 50-800 mg L^{-1} was agitated until the equilibrium was achieved. The adsorbed amounts (q_e) of dye were calculated by the following equation:

$$q_e = \frac{C_0 - C_e}{m} \times V$$

Where C_o and C_e are the initial and equilibrium concentrations of dye in mg L^{-1}, m is the mass of adsorbent (g), and V is the volume of solution (L).

Results and discussion

Adsorbent characterization

Figure 2.a shows the small angle XRD patterns of the fluorene functionalized SBA-15. The sample have a single intensive reflection at 2θ angle around 0.87° similar to the typical SBA-15 materials, that is generally recognized to the long-range periodic [33]. Also two additional peaks related to the higher ordering (110) and (200) reflections are also observed, which is associated with a two-dimensional hexagonal (p6mm) structure [35]. However, in the case of functionalized SBA-15 material, the peak (100) intensity decreases after immobilizations due to the difference in the

scattering difference of the pores and the walls, and to the irregular covering of organic groups on the nanochannels [36].

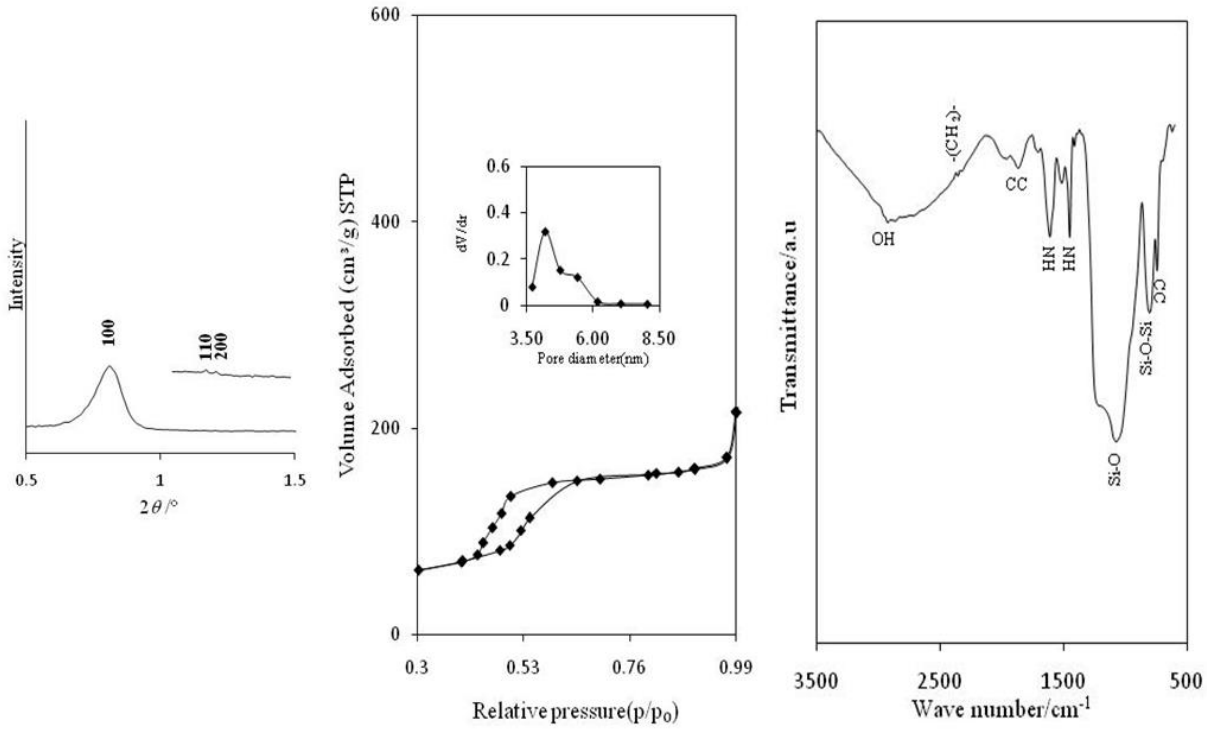

Figure 2. Small angle XRD pattern fluorene functionalized SBA-15(a), Nitrogen adsorption-desorption isotherm of fluorene functionalized SBA-15, (inside: BJH pore size distribution curve of functionalized SBA-15) (b), FT-IR spectrum of fluorene functionalized SBA-15(c).

The textural properties of the sample were evaluated by the nitrogen adsorption-desorption isotherm (Figure 2.b). The material exhibit a typical irreversible type IV nitrogen adsorption isotherm with an H1 hysteresis loop as defined by IUPAC [37]. The nitrogen adsorption at low relative pressures is accounted for by monolayer adsorption of N_2 on the pore walls, and does not essentially involve the presence of micropores. The sharp inflection in the P/P0 range from 0.40 to 0.60 of the isotherm is characterized as capillary condensation within uniform mesopores, the position of which is clearly correlated to a diameter in the mesopore rang. The pore size distribution can be calculated from BJH method based on the desorption branch of the N_2 adsorption isotherm. As demonstrated in Figre. 2.b, a typical BJH plot from modified SBA-15 with fluorene a narrow pore size distribution is observed [38]. The uniformity of the mesopores in this modified SBA-15 is comparable to the SBA-15, indicating that the integrity of the original inorganic wall structure of the SBA-15 is retained. The textural parameters, specific surface areas (BET method), pore diameters (BJH method) and total pore volumes are given in Table 1.

Table 1. The pore diameter (D_{BJH}), BET surface area (S_{BET}) and the total pore volume (V_{total}) from nitrogen adsorption-desorption for the SBA-15 and fluorene functionalized SBA-15.

Molecular sieves	$D_{BJH}(nm)$	$S_{BET}(m^2/g)$	$V_{total}(cm^3/g)$
SBA-15	6.2	587	0.780
Fluorene functionalized SBA-15	4.2	200	0.365

Figure 2.c shows FT-IR spectrum of fluorene modified SBA-15. The bands at 800 and 1086 cm^{-1} are attributed to Si-O-Si and Si-O stretching vibrations, respectively [39]. Also the adsorption bands at 1598 and 1465 cm^{-1} due to N-H bending. The band at 2930 cm^{-1} is assigned to C-H stretching vibrations of the methylene groups. The strong peak of 742 cm^{-1} was observed which due to the C=C ring skeletal vibrations and also the weak peak at 1610 and 1449 cm^{-1} are related to the same type of vibrations.

Figure 3.a shows the Raman spectrum of fluorene modified SBA-15. The band at 2900 cm^{-1} is attributed to C-H stretching in the propyl chain in fluorene modified SBA-15. The strong bands at 1610, 1484 and 1024 cm^{-1} are related to the C-C and C=C ring skeletal vibrations of fluorene. The bands at 3100 and 1350 cm^{-1} are attributed to C-H ring and C-N vibrations, respectively that confirm fluorene was attached on the surface of SBA-15 [40]. The IR and Raman results exhibit that fluorene is attached on the surface of SBA-15.

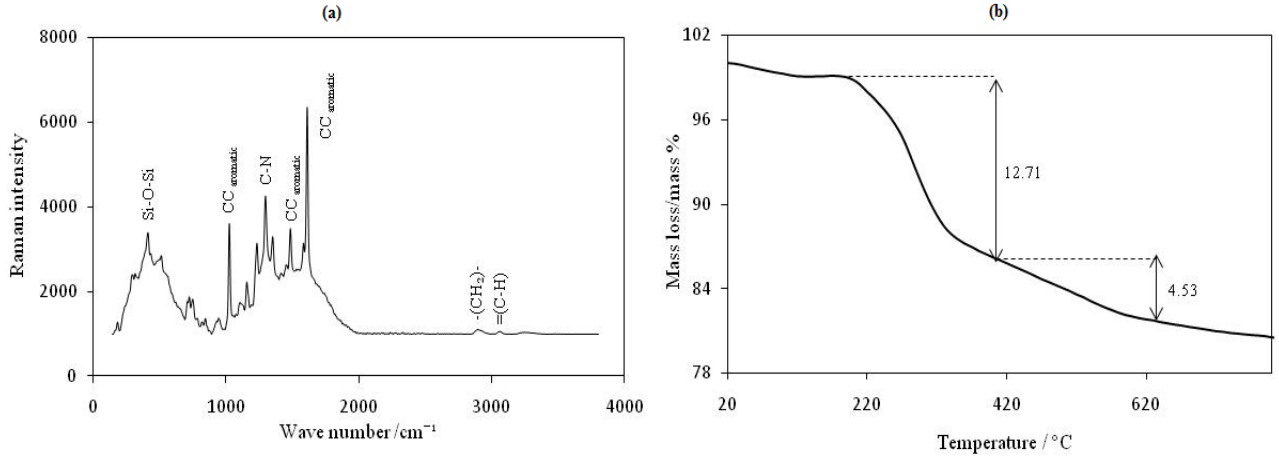

Figure 3. Raman spectrum (a), TGA analysis (b) of fluorene functionalized SBA-15.

Thermogravimetric analysis (TGA) and elemental analysis were carried out to determinate the grafted amount of fluorene incorporated in SBA-15. The TGA profile sample of fluorene functionalized SBA-15 is illustrated in Figure 3.b.

The weights loss at temperature about 100 °C is corresponded to the desorption of physisorbed water that is 1.5% for fluorene modified SBA-15[41]. The weights loss (17.24 %) between 200 and 600 °C are due to the decomposition of organic groups in fluorene modified SBA-15. A minor weight loss due to silanol condensation at high temperature was observed [42]. The experimental and the theoretical C/N molar ratio of fluorene modified SBA-15 was calculated from the elemental analysis data (table 2) which confirms that fluorene is grafted to surface. The TGA is in the good agreement with the organic content determined by elemental analysis.

Table 2. The elemental analysis of fluorene functionalized SBA-15.

Sample	C%	N%	C/N $_{Experimental}$	C/N $_{Theoretical}$	Aminopropyl (mmol /g)	Fluorene (mmol /g)
Fluorene functionalized SBA-15	12.98	1.6	8.1	9.5	1.2	0.55

Effect of pH on the removal yield

The effects of pH 3.0 to 8.0 on the adsorption of dyes are shown in Figure 4. The pH was adjusted by HCl and NaOH and measured by digital pH meter. As depicted in Figure 4, a relatively considerable decrease in the adsorption amount or removal percentage for both of the anionic dyes is occurred under basic conditions. It is attributed to that solution pH may affect both aqueous chemistry and surface binding sites of the adsorbent.

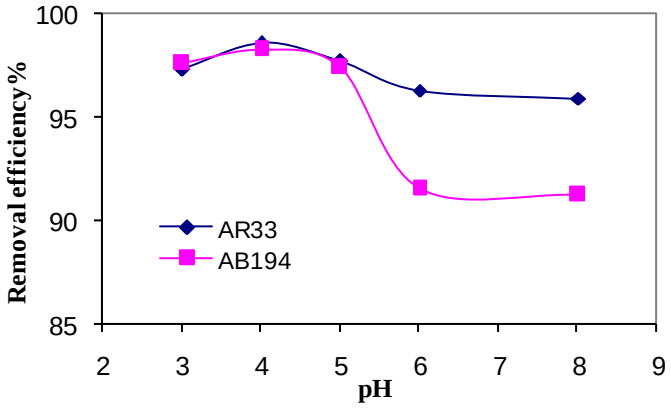

Figure 4. The effect of pH on the adsorption of AR33 and AB194 on the fluorene functionalized SBA-15.

During the dyes adsorption process, different kinds of interactions between SBA-15 grafted with N-(4-(trimethylsilyl)butyl)-9H-fluorene-9-amine and dyes molecules such as physical adsorption, hydrogen bonds, electrostatic attractions, hydrophobic attractions, etc., can act simultaneously. The

aromatic cycles of dyes and fluorene groups of adsorbent could interact with each other by π–π interactions. A great distinction of the acid dyes is the number of hydrophilic functional groups, which have a strong tendency to form hydrogen bonds with fluorene functionalized SBA-15. For example, the azo groups inter act with the silanol groups present on the internal surface of the mesoporous silica by hydrogen bonding. Also, the sulfonic acid groups interact with the positively charged surface of fluorene functionalized SBA-15 by electrostatic interactions. At lower pH, the fluorene functionalized SBA-15 surface will be positively charged via protonation process, which increases the electrostatic attractions between acid dyes molecules and functionalized SBA-15 surface. At higher pH the number of positively charged sites is reduced and raised the number of negatively charged sites, creating electrostatic repulsion between the negatively charged surfaces of the fluorene functionalized SBA-15 and the anionic acid dyes molecules. On the other hand, the lower adsorption of acid dyes, at alkaline pH is because of the presence of excess OH^- ions competing with the dye anions for the adsorption sites. As a result, there was in a significant reduction in the adsorption of acid dyes from the solution. A similar behavior was observed for the adsorption of anionic dye onto amino-functionalized SBA-3 [21].

Effect of the amount of adsorbent on removal efficiency

The effect of the amount of fluorene functionalized nanoporous silica SBA-15 as adsorbent on the removal of acidic dyes was determined at room temperature and at pH 4.0 by varying the adsorbent amount from 0.003 to 0.020 g in 10 mL solution of 50 mg L^{-1} of each dye. The results show (Figure 5.a) that the removal efficiency of dyes initially was increased by increasing the amount of adsorbent due to the availability of higher adsorption sites. Then the percentage removal reaches almost a constant value. The 5 mg functionalized SBA-15 had a removal efficiency of 99% for AR33 and 96% for AB194, while 10 mg functionalized SBA-15 had a removal efficiency of more than 99% for both of them. It can be attributed to the more sulfonic acid groups of AR33 dye which increases electrostatic interactions among AR33 and functionalized SBA-15.

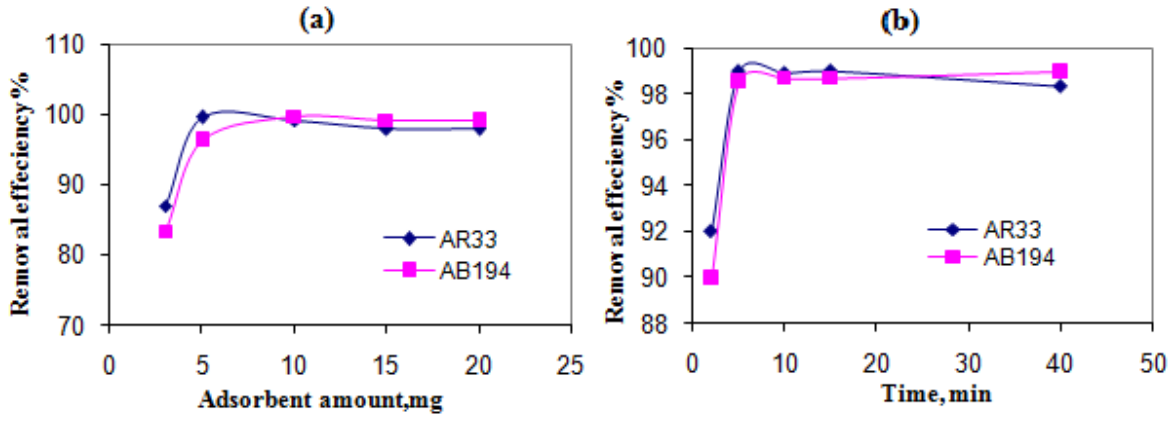

Figure 5. The effect of different amount of fluorene functionalized SBA-15(a), and contact time (b) on percentage of AR33 and AB194 dye removal.

Effect of contact time on removal yield

The effect of contact time on the amount of dyes adsorbed was investigated at the initial concentration of 50 mg L^{-1} of dyes at pH 4.0 at room temperature. The concentration of dyes was measure periodically in 2, 5, 10, 15, and 40 minutes. Figure 5.b shows the effect of contact time on the removal yield of dyes by the fluorene functionalized nanoporous silica SBA-15. It can be seen that after about 5 min, almost whole of the dye has been adsorbed. Therefore, contact time of 5 min was selected for further works.

Effect of initial dye concentration

A higher initial acid dye concentration leads to an increase in the mass gradient between the solution and the adsorbent, which then functions as a driving force for the transfer of acid dye molecules from bulk solution to the adsorbent surface [21]. Effect of initial concentration on the uptake of acid dyes was studied at different initial concentrations (50, 100, 300, 500 and 800 mg/L). As can be seen in Figure 6, the amount of dyes adsorbed increases as the concentration increases up to a saturation point. As long as there are available sites, adsorption will increase with increasing dye concentrations, but as soon as all of the sites are occupied, a further increase in concentrations of dyes does not increase the amount of dyes on adsorbents.

The higher values of (q_e) for AR33 than that for AB194 in whole of concentration range indicated its more interaction with fluorene modified SBA-15.

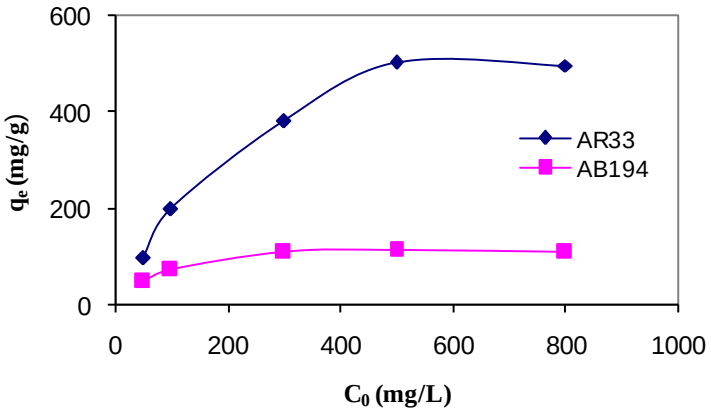

Figure 6. The Langmuir adsorption isotherm of AR33 (a) and AB194 (b) on fluorene functionalized SBA-15.

Adsorption isotherms

In order to optimize the use of fluorene functionalized SBA-15, it is important to establish the most

appropriate adsorption isotherm. The principle of adsorption isotherms is to find the relation-ship between the mass of the solute adsorbed per unit mass of adsorbent qe (mg/g) and the solute concentration in the solution at equilibrium Ce (mg/L). The adsorption capacities of the as-obtained functionalized SBA-15 to dyes were measured individually at pH 4.0 with 10.0 mL varied AR33 and AB194 concentrations. Equilibrium isotherms were analyzed by Freundlich and Langmuir isotherm models. The Freundlich isotherm is derived by assuming a heterogeneous surface with a non-uniform distribution of heat of adsorption over the surface. Whereas, in the Langmuir theory, the basic assumption is that the sorption takes place at specific homogeneous sites within the adsorbent.

The linearized form of the Langmuir is [43]:

$$\frac{C_e}{q_e} = \frac{1}{bq_m} + \frac{C_e}{q_m}$$

Where q_m is the maximum adsorption capacity corresponding to complete monolayer coverage and b is the equilibrium constant (L/mg). The data fit well to the model with correlation coefficients (R^2) in the range of 0.993 and 0.998 for AR33 and AB194 respectively (Table 3).

The Freundlich model can take the following linearized form [44]:

$$logq_e = logk_f + \frac{1}{\mathrm{n_f}} logC_e$$

Where K_f is is roughly an indicator of the adsorption capacity and $1/n_f$ is the adsorption intensity. The slope $1/n_f$ ranging between 0 and 1 is a measure of adsorption intensity or surface heterogeneity, becoming more heterogeneous as its value gets closer to zero [45].

Table 3. Isotherm parameters for adsorption of acid dyes on fluorene functionalized SBA-15.

Dyes	Langmuir			Freundlich		
	q_m(mg g^{-1})	b(L mg^{-1})	R^2	K_f(mg g^{-1})	1/n	R^2
AR33	500	0.0392	0.993	120.22	0.223	0.839
AB194	110	0.1893	0.998	42.46	0.143	0802

The constants are determined by using linear regression analysis and are presented in Table 3. As seen from Table 3, the Freundlich model is not suitable for describing the adsorption equilibrium of dyes by functionalized SBA-15 and Langmuir isotherm model yielded the best fit with the highest R^2 value compared to the Freundlich model.

Also as the results show, the maximum adsorption capacities in the studied concentration range are 500.0 mg/g and 110.0 mg/g for AR33 and AB194, respectively. The capacity factor of adsorbent for

AR33 is higher than that for AB194. The differences may be due to the differences in the structure of dyes. AR33 and AB194 are anionic dyes because of they usually exist in the sulphate form. Two sulphate groups in AR33 increase the electrostatic attractions between acid dye molecule and fluorene functionalized SBA-15 surface. Therefore, the adsorption capacity of fluorene functionalized SBA-15 for AR33 seems to be better than it for AB194 dye with one sulphate group.

Desorption and reuse study

The reusability of adsorbent is of great importance as a cost effective process in water treatment. In order to regenerate and reuse the functionalized SBA-15 after adsorbing dyes, 15 mL of 2.0 M sodium hydroxide solution was selected as the regeneration agent. Three cycles of adsorption-desorption studies were accordingly carried out. It is notable that the equilibrium of desorption was achieved rapidly within about 5 min, similar to the adsorption equilibrium. After the elution of the adsorbed dyes, the adsorbent was washed with DDW and dried under vacuum at 25°C and reused for dyes removal. The adsorption capacity of the sorbent after three cycles was reduced only 10%, which was due to the incomplete desorption of dyes. Therefore, the fluorene functionalized SBA-15 can be a good reusable and economical sorbent.

Removal of dyes from dyeing wastewater sample

The application of the AR33 and AB194 dyes removal from real sample was examined by dyeing wastewater of handmade carpet's fibers. Because of matrix effect, the initial concentration and residual concentration of dyes in the samples (before and after removal with the recommended procedure) was determined by standard addition method. The results are given in Table 4. As shown, the proposed method could be applied successfully for the removing of AR33 and AB194 dyes in wastewater samples with very good efficiency.

Table 4. Removal of AR33 and AB194 dyes from dyeing wastewater sample.

Dyes	Initial concentration (mg L^1)	Final concentration (mg L^1)	%Removal
AR33	24.83(± 0.52)[a]	0.67 (± 0.51)	97.30 (± 0.67)
AB194	19.50 (± 0.54)	0.50 (± 0.48)	97.43 (± 0.65)

[a] %RSD based on three replicate analysis

Comparison of other adsorbents

The dye adsorption capacity data on the application of previously developed adsorbent for removing Acid dyes [21, 46-49] were summarized in Table 5 and compared with those of the SBA-15 grafted with N-(4-(trimethylsilyl) butyl)-9H-fluorene-9-amine.

Table 5. Comparison of various adsorbents used for removal of Acid dyes.

Adsorbent	Dye	Adsorption capacities (mg/g)	Contact Time (min)	Ref.
Pentaethylene hexamine functionalized SBA-3	Acid Green 28, Acid Yellow 127, Acid Orange 67, Acid Red 114, Acid Blue 113	285.71, 476.19, 434.78, 454.54, 500	60	21
Magnetic chitosan-Fe(III) hydrogel	Acid Red 73,	294.5	10	46
Activated rice husk carbon	Acid yellow 36	86.9	90	47
Activated carbon	Acid Red 97	82.08	20	48
Multiwalled carbon nanotubes	Acid Red 18	166.67	120	49
SBA-15 grafted with N-(4-(trimethylsilyl)butyl)-9H-fluorene-9-amine	Acid Red 33, Acid Black 194	500.0, 110.0	5	This work

It can be seen that the adsorption capacity of modified adsorbent exceed those of most of previously reported adsorbents. It is noteworthy that adsorbent also less adsorption capacities in comparison with some previous reports. Yet, in terms of the optimal contact time it excel the best previously reported adsorbent.

Conclusion

This work has demonstrated the successful application of SBA-15 grafted with N-(4-(trimethylsilyl)butyl)-9H-fluorene-9-amine for the removal of acidic dyes. The adsorbent was very effective in removing Acidic dyes and the adsorption of dyes to functionalized SBA-15 was agreed well to the Langmuir adsorption model with maximum adsorption capacities of 500.0 and 100 mg/g for AR33 and AB194, respectively.

The adsorption of dyes to fluorene functionalized SBA-15 was fast, which could reach equilibrium in less than 5 min. Since the adsorption capacities of fluorene functionalized SBA-15 is good (a low amount of it is enough for high efficiency removal) and the preparation of fluorene functionalized SBA-15 is easy, this methodology could be suitable for the large scale removal of the pollutant dyes from water and wastewater.

Acknowledgement

The author thanks the Islamic Azad University of Yadegar-e-Imam Khomeini (RAH) shahre-rey branch research council for support of this work.

References

[1] S. Qadri, A. Ganoe, Y. Haik, *J. Haz. Mater*., 169, 318 (2009).

[2] S. Qu, F. Huang, S. Yu, G. Chen, J. Kong, *J. Haz. Mater.*, 116, 643 (2008).

[3] S. Chen, J. Zhang, C. Zhang, Q. Yue, Y. Li, C. Li, *Desalination*, 252, 149 (2010).

[4] F. Ferrero, *J. Environ. Sci*., 22, 467 (2010).

[5] L. Li, S. Liu, T. Zhu, *J. Environ. Sci.*, 22, 1273 (2010).

[6] A. Mittal, V.K. Gupta, A. Malviya, J. Mittal, *J. Hazard. Mater*., 151, 821 (2008).

[7] S.H. Chang, K.S. Wang, H.C. Li, M.Y. We, J.D. Chou, *J. Hazard. Mater*., 172, 1131 (2009).

[8] K. Zhao, G. Zhao, P. Li, J. Gao, B. Lv, D. Li, *Chemosphere*, 80, 410 (2010).

[9] J. Rajeev, M. Megha, S. Shalini, M. Alok, *J. Environ. Manage*., 85, 956 (2007).

[10] R. Malik, D.R. Ramteke, S.R. Wate, *Waste Manage*., 27, 1129 (2007).

[11] E. Forgacs, T. Cserhati, G. Oros, *Environ. Int*., 30, 953 (2004).

[12] P.V. Messina, P.C. Schulz, *J. Colloid Interface Sci*., 299, 305 (2006).

[13] S. Wang, Z.H. Zhu, *J. Hazard. Mater. B*, 136, 946 (2006).

[14] X.S. Zhao, G.O. Lu, X. Hu, *Microp. Mesop. Mater*., 41, 37 (2000).

[15] D. Perez-Quintanilla, A. Sanchez, I. Del Hierro, M. Fajardo, I. Sierra, *Microchim. Acta*, 165, 291 (2009).

[16] M.R. Ganjali, L. Hajiaghababaei, A.R. Badiei, K. Saberyan, M. Salavati-Niasari, G.M. Ziarani, S.M.R. Behbahani, *Quimica Nova*., 29, 440 (2006).

[17] M.R. Ganjali, L. Hajiaghababaei, A.R. Badiei, G. Mohammadi Ziarani, A. Tarlani, *Anal. Sci.*, 20, 725 (2004).

[18] M.H. Lim, A. Stein, *Chem. Mater*., 11, 3285 (1999).

[19] K.Y. Ho, G. Mckay, K.L. Yeung, *Langmuir*, 19, 3019 (2003).

[20] M. Anbia, S. Asl Hariri, S.N. Ashrafizadeh, *Appl. Surface Sci*., 256, 3228 (2010).

[21] M. Anbia, S. Salehi, *Dye. Pigment*., 94, 1 (2012).

[22] Y. Gan, N. Tian, X. Tian, L. Ma, W. Wang, C. Yang, Z. Zhou, Y. Wang, *J. Porous Mater*., 22, 147 (2015).

[23] Y. Li, Y. Zhou, W. Nie, L. Song, P. Chen, *J. Porous Mater*., 22, 1383 (2015).

[24] Y.H. Ju, O.F. Webb, S. Dai, J.S. Lin, C.E. Barnes, *Ind. Eng. Chem. Res*., 39, 550 (2000).

[25] B. Lee, L.L. Bao, H.J. Im, S. Dai, E.W. Hagaman, J.S. Lin, *Langmuir*, 19, 4246 (2003).

[26] G.E. Fryxell, J. Liu, T.A. Hauser, Z. Nie, K.F. Ferris, S. Mattigod, M. Gong, R.T. Hallen, *Chem. Mater*., 11, 2148 (1999).

[27] A. Badiei, P. Norouzi, F. Tousi, *Europ. J. Sci. Res*., 12, 39 (2005).

[28] A. Badiei, L. Bonneviot, N. Crowther, G. Mohammadi Ziarani, *J. Organomet. Chem*., 691, 5923 (2006).

[29] D. Zhao, J. Feng, Q. Huo, N. Melosh, G. Fredrckson, B. Chmelka, G.D. Stucky, *Science,* 279, 548 (1998).

[30] W.L.F. Armarego, D.D. Perrin, Purification of Laboratory Chemicals, Elsevier, (1996).

[31] A. Badiei, H. Goldooz, G. Mohammadi Ziarani, *Appl. Surf. Sci*., 257, 4912. (2011).

[32] S. Hamoudi, A. El-Nemr, K. Belkacemi, *J. Coll. Interf. Sci*., 343, 615 (2010).

[33] D.Y. Zhao, Q.S. Huo, J.L. Feng, B.F. Chmelka, G.D. Stucky, *J. Am. Chem. Soc*., 120, 6024 (1998).

[34] J.R. Sampay, E. Emmet Reid, *J. Am. Chem. Soc*., 69, 234 (1947).

[35] D. Zhao, J. Feng, Q. Huo, N. Melosh, G.H. Fredrickson, B.F. Chmelka, G.D. Stucky, *Science*, 279, 548 (1998).

[36] M. Kruk, M. Jaroniec, C.H. Ko, R. Ryoo, *Chem. Mater*., 12, 1961 (2000)

[37] K.S.W. Sing, D.H. Everett, R.A.W. Haul, L. Moscou, R.A. Pierotti, J. Rouquerol, T. Siemieniewska, *Pure Appl. Chem*., 57, 603 (1985).

[38] M. Yadavi, A. Badiei, G.M. Ziarani, A. Abbasi, *Chem. papers*., 67, 751 (2013).

[39] G. Socrates, Infrared and Raman Characteristic Group Frequencies, John Wiely (2004).

[40] M. Yadavi, A. Badiei, G.M. Ziarani, *Appli. Surf. Sci*., 279, 121 (2013).

[41] C.P. Jaroniec, M. Kruk, M. Jaroniec, A. Sayari, *J. Phys. Chem. B,* 102, 5503 (1998).

[42] L.T. Zhuravlev, *Coll. Surf.*, 1, 173 (2000).

[43] I., Langmuir, *J. Am. Chem. Soc*., 40, 136 (1918).

[44] H.M.F. Freundlich, *J. Phys. Chem*., 57, 385 (1906)

[45] F. Haghseresht, G. Lu, *Energy Fuels,* 12, 1100 (1998).

[46] C. Shen, Y. Shen, Y. Wena, H. Wang, W. Liu, *water Res.*, 4, 5200 (2011).

[47] A. Tor, Y. Cengeloglu, *J. Hazard. Mater.*, 138, 409 (2006).

[48] V. Gomez, M. S. Larrechi, M. P. Callao, *Chemosphere*, 69, 1151 (2007).

[49] M. Shirmardi, A. Mesdaghinia, A. H. Mahvi, S. Nasseri, R. Nabizadeh, *E-J. Chem.*, 9, 2371 (2012).